One-click Self-Healing Elastomer with Closed-Loop Recyclability

Justin Jian Qiang Mah [1,2]†, Ke Li[1]†, Hongzhi Feng[3,4], Nayli Erdeanna Binte Surat'man[3], Bofan Li[3], Xiaohui Yu[3,5], Mingsheng Zhang[1], Sheng Wang[3*], Zibiao Li[1,3,5*]

[1] Institute of Materials Research and Engineering (IMRE), Agency for Science, Technology and Research (A*STAR), 2 Fusionopolis Way, Innovis #08-03, Singapore 138634, Republic of Singapore

[2] Division of Chemistry and Biological Chemistry, School of Physical and Mathematical Sciences, Nanyang Technological University, Singapore 637371, Republic of Singapore

[3] Institute of Sustainability for Chemicals, Energy and Environment (ISCE[2]), Agency for Science, Technology and Research (A*STAR), 1 Pesek Road, Jurong Island, Singapore 627833, Republic of Singapore

[4] Key Laboratory of Bio-based Polymeric Materials Technology and Application of Zhejiang Province, Laboratory of Polymers and Composites, Ningbo Institute of Materials Technology and Engineering, Chinese Academy of Sciences, Ningbo 315201, P. R. China

[5] State Key Laboratory for Modification of Chemical Fibers and Polymer Materials, College of Materials Science and Engineering, Innovation Center for Textile Science and Technology, Donghua University, Shanghai 201620, P. R. China

[6] Department of Materials Science and Engineering, National University of Singapore, 9 Engineering Drive 1, Singapore 117576, Republic of Singapore

* Correspondence to wang_sheng@isce2.a-star.edu.sg (S. Wang); lizb@imre.a-star.edu.sg (Z. Li)

† These authors contributed equally to this work

KEYWORDS: One-click self-healing, elastomer, closed-loop recycling

Abstract

The loss of function after prolonged periods of use is inevitable for all materials including plastics. Hence, self-healing capabilities are a key development to prolong the service lifetime of materials. One of such self-healing capabilities can be achieved by integrating dynamic bonds such as boronic ester linkages into polymeric materials, however the rate of self-healing in these materials is insufficient and current methods to accelerate it are limited. In this study, we report the design, synthesis and characterization of a fluorinated elastomer (FBE15) that utilizes enhanced interaction between polymer chains afforded by strong dipole-dipole interactions from $-CF_3$ side chains which showed an increase in binding energy to -7.71 Kcal/mol from -5.51 Kcal/mol, resulting in increased interaction between the boronic ester linkages and improving self-healing capabilities of boronic ester materials, drastically reducing the time required for stress relaxation from 9 min to 1 min. The bulk elastomer is capable of ultrafast self-healing in a one-click fashion that can happen in mere seconds, which can then be stretched to 150 % of its original length. By utilising the dynamic cross-linking, FBE15 is also capable of mechanical reprocessing, and chemical recycling into its starting linear polymer and cross-linker, allowing reformation of the material that has comparable properties to the original at the end of its service lifespan.

1. Introduction

Plastic materials have since become ubiquitous in modern society, being one of the most produced materials worldwide. However, all materials gradually experience loss of function resulting from wear after prolonged use and plastic materials are no exceptions. The problem is compounded by the fact that conventional plastic materials are largely non-recyclable, leading to large amounts of plastic waste generated every year. As such, materials that mimic biological organisms' ability to repair itself has garnered significant attention over the years.

Dubbed self-healing materials, these materials respond to physical or chemical stimulus, triggering an event that repairs itself on the molecular level. The mechanism of action can be broadly classified as either extrinsic or intrinsic.[1] Extrinsic self-healing relies on embedded catalysts and monomers that undergo polymerization or cross-linking upon damage, thereby replacing the damaged portion with new polymers or cross-links. While straightforward and reliable, the downside to extrinsic self-healing is that it is limited by the amount of embedded monomers which decreases after each healing cycle, resulting in eventual loss of self-healing properties. On the other hand, intrinsic self-healing is enabled by the rearrangement of its dynamic intermolecular forces or covalent bonds within the polymer, which restores the polymer upon damage. Theoretically, intrinsic self-healing would be repeatable with no limit on the healing cycles since it does not rely on additional reactants, however a stimulus may still be needed depending on the type of intermolecular force or dynamic covalent bond incorporated.[2, 3]

Thus far, intrinsic self-healing materials have been developed using several dynamic interactions and bonds, such as hydrogen bonds[4-6], host-guest interactions[7-9], metal-ligand interactions[10-12], boronic and boronate esters[13-20], disulfide linkages[21, 22], Diels-Alder adducts[23-26] and imine bonds[27-29]. The multitude of self-healing mechanisms available allows tuning of the material's mechanical properties and self-healing capabilities by the choice of dynamic interactions and bonds. Materials containing boronic esters are interesting as it is possible to self-heal at ambient conditions as the topology freezing transition temperature is often below room temperature which allows for bond exchange to occur at room temperature.[30] Boronic esters also imparts strong covalent linkages to the polymer matrix which undergoes dynamic exchange via both associative and dissociative mechanisms in the presence of free -OH groups or moisture respectively.[31]

Evidently, the self-healing capabilities of such materials is an important property to be considered in assessing the bulk material's reusability. Early reports of a self-healing boronic ester bulk material by Sumerlin and co required 4 days to heal from damage[13], while subsequent reports by Chen et al was able to reduce the self-healing duration to 24 h although it required a temperature of 80 °C to accelerate the process.[32] More recently, a boronic ester vitrimer made from epoxidized soybean oil acrylate was reported to be able to heal from damage in 24 h at room temperature, which was significantly faster than its predecessors, although the improvement was not investigated but can be attributed to the high mobility of the polymer due to its low glass transition temperature (T_g).[33] On the other hand, the inclusion of neighbouring electron donating moieties that can form B-N coordination bonds have also been found to accelerate the rate of self-healing similar to boronate ester linkages or being in a basic environment.[14, 34, 35] Lastly, the effects of adjacent hydroxyl groups was investigated and found

to be able to participate and accelerate the exchange of B-O bonds which increased the healing efficiency of the boronic ester material from 10 % after 48 h to 81 % after 12 h.[36]

Due to the limited methods available of accelerating the self-healing of boronic ester containing materials and the extended amount of time required to heal such materials under ambient conditions, the development of alternative methods to improve on the self-healing capabilities is a desirable outcome to realize the deployment of such materials in real-life applications. To achieve that, we considered the inclusion of a secondary self-healing mechanism which have been reported to afford a change in properties of such self-healing materials[37-40], to be a promising method to improve on the self-healing capabilities of materials containing boronic esters.

We hypothesize that the inclusion of a secondary self-healing system could accelerate the bond exchange of boronic esters due to increased interaction or activity, allowing the material to heal at an increased rate that is not present in individual self-healing systems. In this study, we describe the design and characterization of a fluorinated elastomer that combines boronic ester linkages and dipole-dipole interaction from CF_3 side chains that is capable of rapid one-click self-healing at ambient conditions, which is not present in the polymer with no -CF_3 moieties. The material can also be mechanically reprocessed and chemically recycled to reform the bulk elastomer with no significant difference in structure and properties, which is an important step towards achieving material circularity and sustainable polymer production.

2. Results and Discussion

2.1 Dual self-healing elastomer design and synthesis

In order to obtain a material with dual self-healing effects, we sought to combine boronic ester linkages with a strong dipole-dipole interaction such as CF_3–CF_3 interactions which was demonstrated to be capable of autonomous self-healing.[41] Hence a vinyl alcohol monomer 2-hydroxyethyl acrylate (HEA) was randomly copolymerized with fluorinated vinyl monomer 2,2,2-trifluoroethyl acrylate (TFEA) using free-radical polymerization with AIBN as an initiator to obtain a linear fluorinated random copolymer (LFP15) bearing 15 % -OH and 85 % -CF_3 side chains, in which the -OH groups can be dynamically cross-linked with boronic acids (outlined in Figure 1).

LFP15 was characterized with gel permeation chromatography (GPC), Fourier-transform Infrared spectroscopy (FTIR), and ^{1}H nuclear magnetic resonance (^{1}H NMR) to confirm the inclusion of HEA and TFEA in the linear polymer. The presence of O-H stretching peaks and C-F stretching at 3500 cm^{-1} and 1280 cm^{-1} in the FTIR spectrum (Figure 2a & 2b) indicates the presence of both -OH and -CF_3 moieties from HEA and TFEA respectively. Similarly, proton signals corresponding to HEA at 3.78 ppm (CH_2–OH), 4.19 ppm (CH_2–OOC), and TFEA at 4.47 ppm (CH_2–CF_3) were observed in the ^{1}H NMR spectrum as well, with the ratio of 3.78 ppm signal and 4.47 ppm being 15:85 (Figure 2c), thus confirming the successful polymerization of LFP15. The LFP15 generated in this manner could be purified in excellent yields of 87 % are approximately 27 kDa in size with a polydispersity index of 3.31 which is expected of free-radical substitutions (Figure 2d).

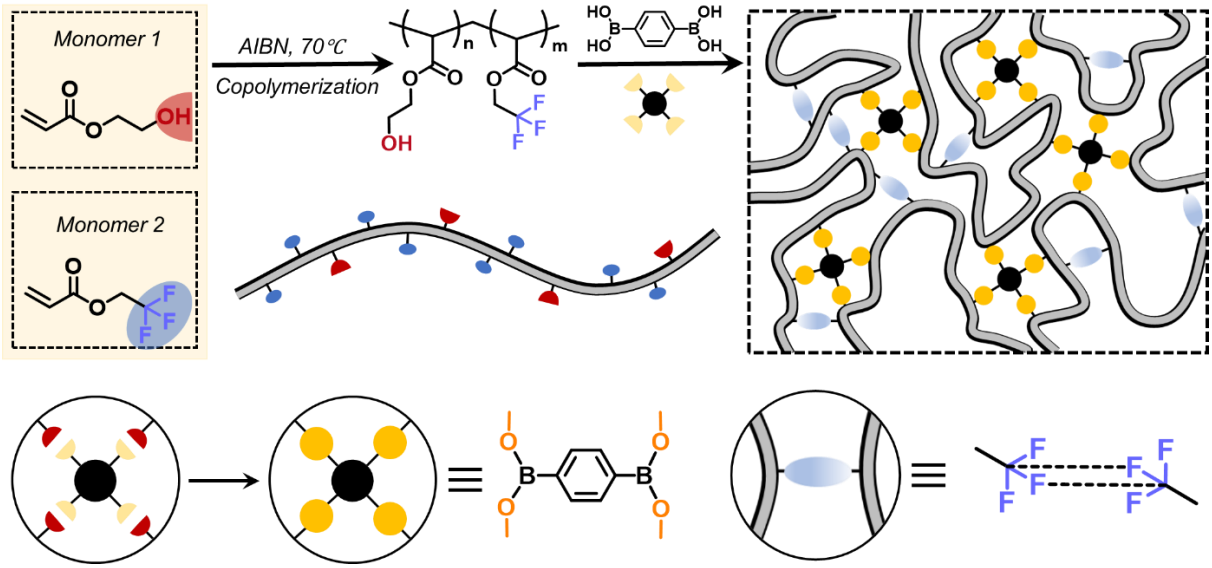

Figure 1. Synthetic route of random copolymer LFP15 and illustration of dynamic cross-linking and dipole-dipole interactions in FBE15.

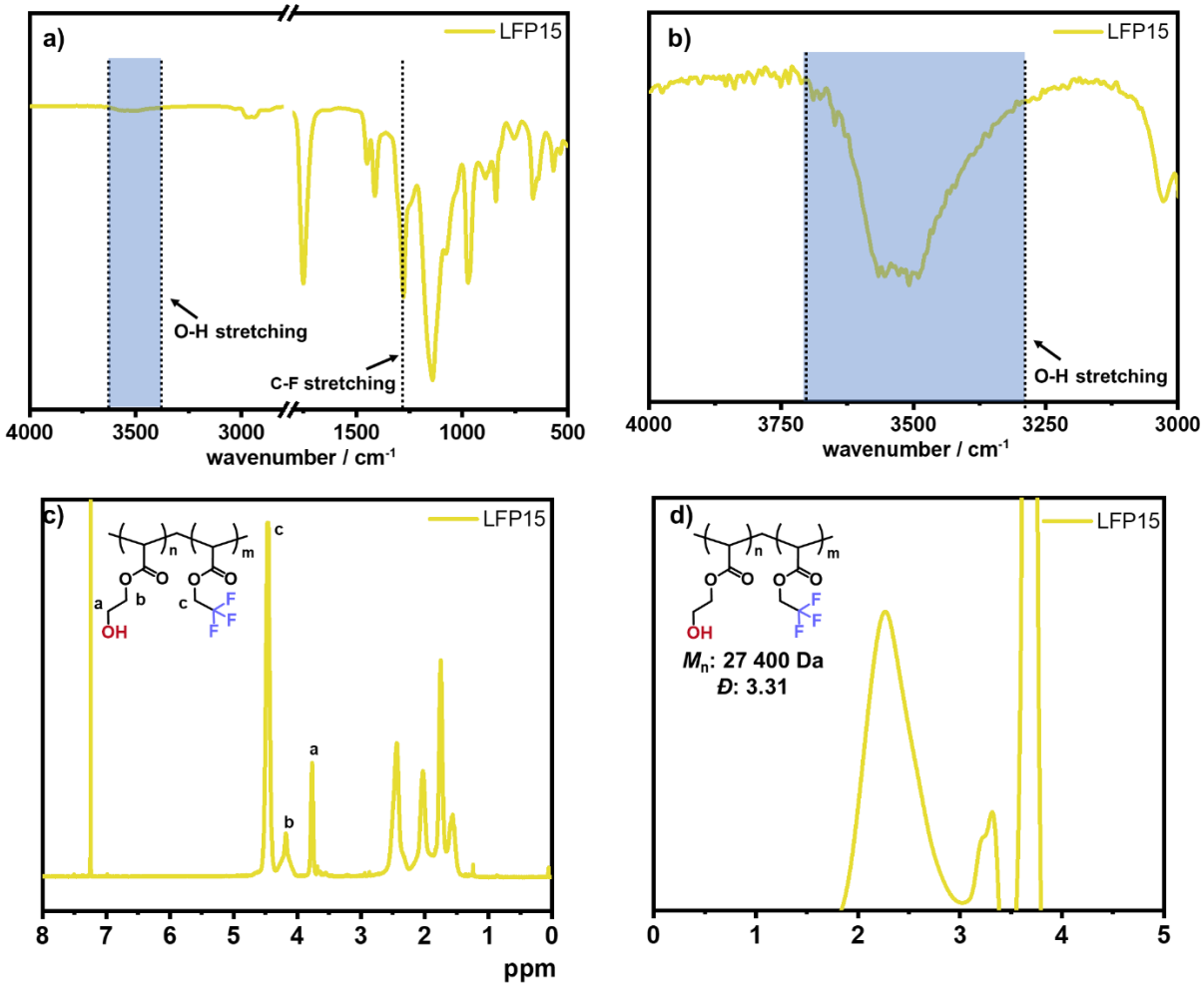

Figure 2. Molecular characterizations of LFP15. (a) FTIR spectrum of LFP15 with O-H and C-F stretching highlighted; (b) Zoomed in FTIR spectrum of LFP15 for O-H stretching (3000 – 4000 cm^{-1}); (c) ^{1}H NMR spectrum of FLP15 in $CDCl_3$ solvent (d) GPC trace of LFP15 (THF eluent, 1.0 mL / min flow rate, 40 °C column temperature, polystyrene standard).

1,4-phenylenebisboronic acid was then added to cross-link LFP15 to reach 15 % cross-linking overall to obtain the fluorinated elastomer (FBE15) as a soft flexible material. FBE15 was characterized with FTIR, XPS and SEM analysis (Figure 3) to confirm the reaction of -OH in LFPs with 1,4-phenylenebisboronic acid. The signal at 1038 cm^{-1} in FTIR spectrum corresponds to the B-O-C of the boronic ester (Figure 3a), while the characteristic binding energy of boron was observed in the XPS scan at 188 eV together with oxygen at 530 eV and fluorine 685 eV (Figure 3b). Similarly, the surface scan of FBE15 using SEM-EDS (Figure S1) reveals the presence of boron, oxygen and fluorine uniformly spread throughout the surface at 8.28 %, 15.4 % and 2.53 % respectively (Figure 3c & 3d), signifying successful formation of boronic ester in FBE15, while the low percentage of fluorine observed in SEM-EDS surface scan is likely due to the migration of fluorine due to repulsion from the electron beam, resulting in a lower observed presence of fluorine which was previously reported by Vandi et al.[42]

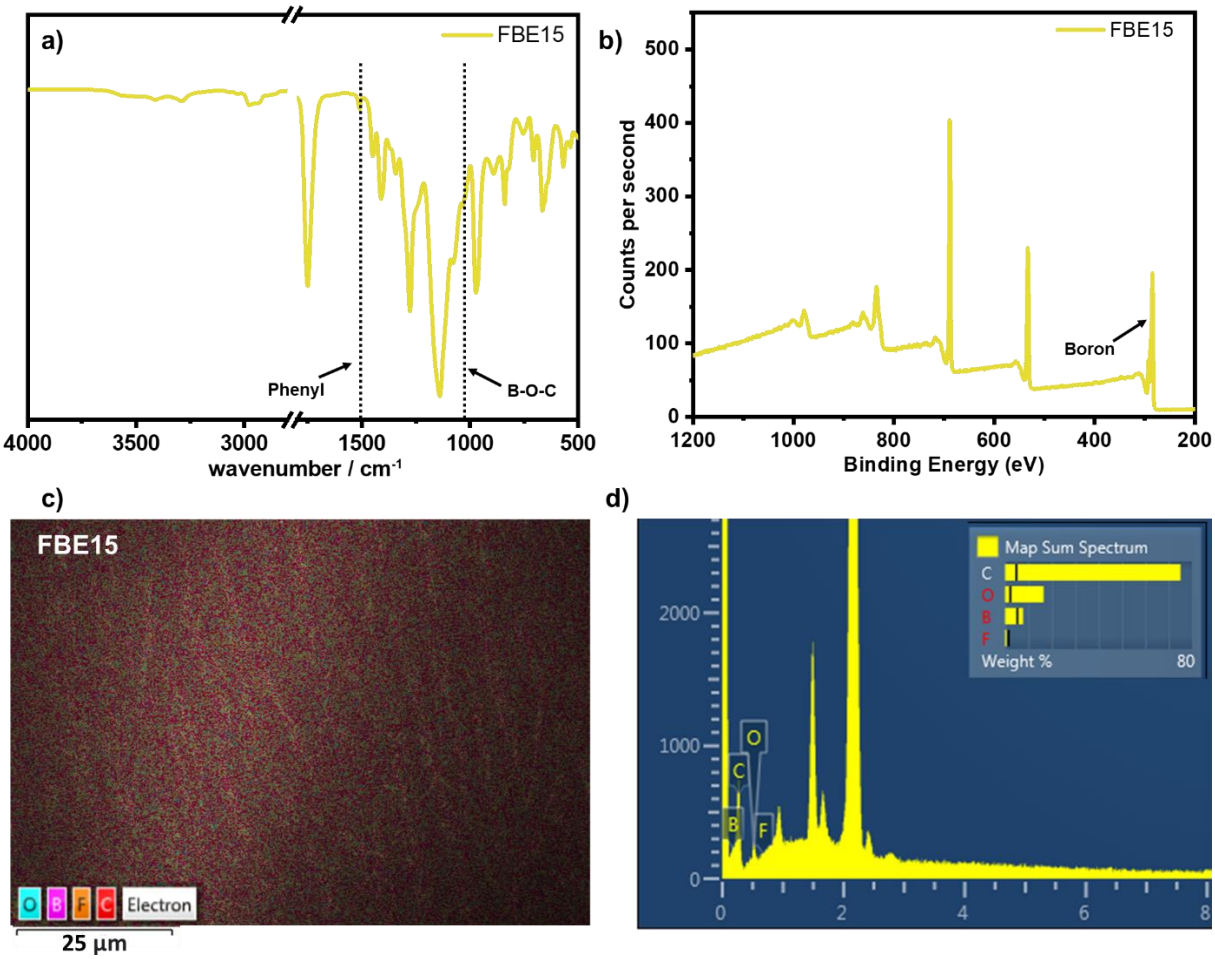

Figure 3. Characterization of FBE15. (a) FTIR spectrum of FBE15 with phenyl and B-O-C signals in boronic ester highlighted; (b) XPS spectra of FBE15 with boron's binding energy annotated; (c) SEM-EDS surface scan of FBE15 with atom overlayed image of O, B, F & C atoms (1000x magnification); (d) Element composition of FBE15 surface calculated from the SEM-EDS scan.

2.2 Thermal properties of FBE15

The thermal properties of FBE15 were evaluated by TGA, DSC and DMA (Figure 4). The initial degradation temperature $T_{d5\%}$ (temperature at which 5 % weight loss occurred) of FBE15 in nitrogen atmosphere was determined to be 287 °C, which was subsequently raised to between 328 °C after cross-linking into the respective FBE15, with no residual carbon left at 600 °C, indicating a good degree of thermal stability for FBE15 (Figure S2). As for its glass

transition temperature (T_g), LFP15 displayed a low T_g of 3.41 °C which increases to 12.4 °C after cross-linking, which is expected as the polymer chains are less mobile after cross-linking in FBE15. The low T_g of FBE15 is optimal to facilitate self-healing under ambient conditions due to the flexible side chains that are free to rearrange in the material.

The storage modulus (E') curve of the FBE15 indicates that the materials follow a temperature-dependent viscoelastic behaviour with a E' of 1600 MPa in its glassy state, which decreases to 1.37 MPa in its rubbery state (T_g + 30 °C). Under an applied strain of 10 %, FBE15 was able to rapidly relax to 1/e of the initial stress in a minute at room temperature, indicating a high bond exchange activity in FBE15 even at room temperature, which is ideal for self-healing materials. Based on the stress relaxation analysis conducted at increasing temperatures, it was observed that the stress relaxation time of FBE15 follows an Arrhenius relationship, with a determined activation energy (E_a) of 39.8 kJ/mol which is in agreement with other reported materials with boronic ester linkages.[43, 44] The topology freezing transition temperature of the material was determined to be 5.5 °C by the extrapolation of the Arrhenius fitted line to when the stress relaxation time (τ^*) was 2.5×10^6 s, which is similar to Zhao et al's reported work (6.4 °C).[30]

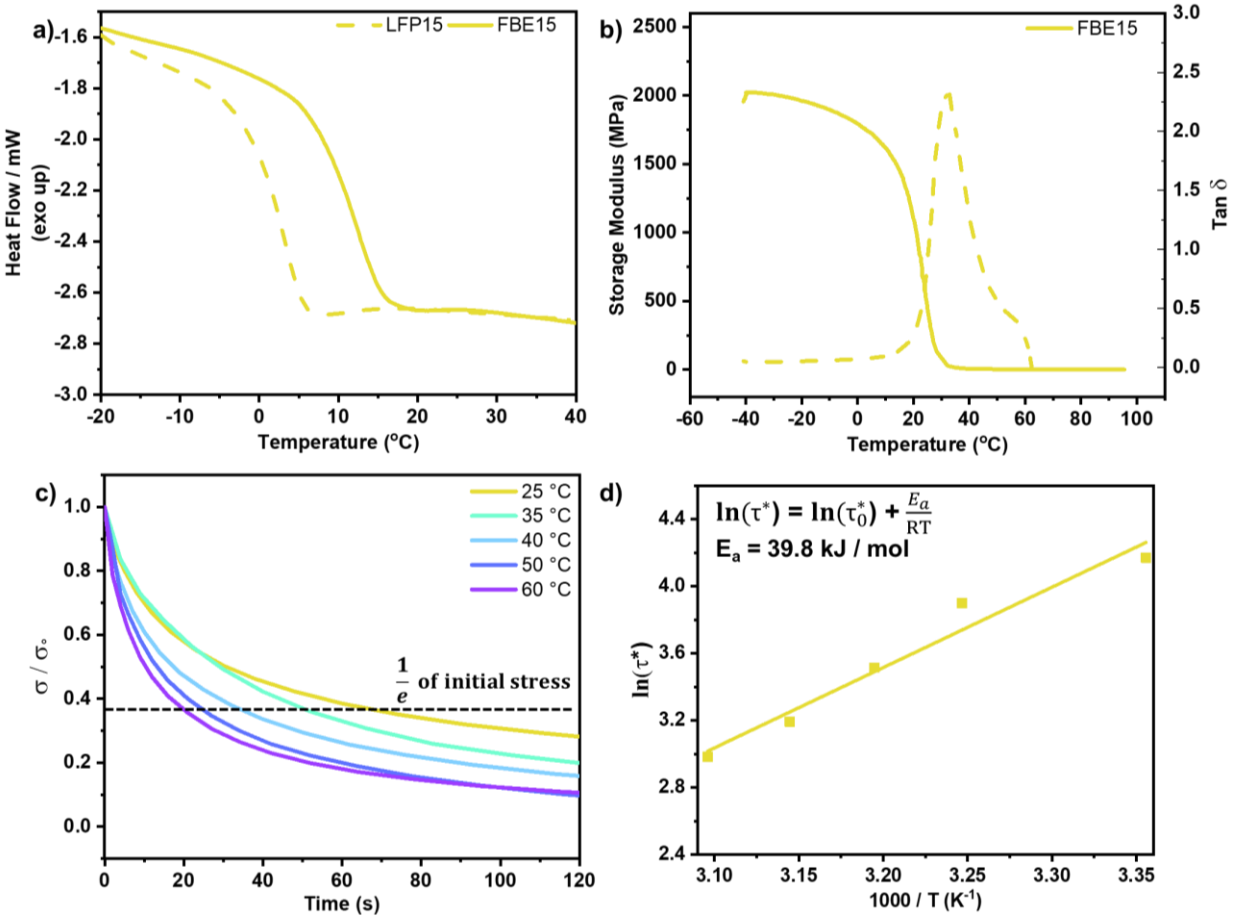

Figure 4. (a) DSC thermogram of LFP15 (dash line) and FBE15 (solid line), (b) Plot of storage modulus (solid line) and tan δ (dash line) against temperature for FBE15, (c) Stress relaxation curve of FBE15 at varying temperatures from 25 °C to 60 °C, (d) Arrhenius fitted curve of relaxation time against 1000/T with E_a of 39.8 kJ/mol.

2.3 Self-healing capabilities of FBE15 and effect of -CF_3 moiety

Similar to the rapid stress-relaxation observed at room temperature, the self-healing capabilities of FBE15 could be demonstrated on the bulk material as well (Figure 5). A 4 cm strip of FBE15 was cut into two, and rejoined by pressing the two halves together in a one-click fashion, the one-clicked self-healed FBE15 could be stretched to 150 % of its original length before breakage (Figure 5a). A similar strip of FBE15 that was cut and pressed together for a minute

could be used to support a weight of 500 g before elongation and eventual breakage (Figure S3), which demonstrates the rapid self-healing even on the bulk material scale. Tensile test was then conducted at a stretching rate of 60 mm/min to compare between a pristine FBE15 sample and one that was cut and healed for 5 min, the pristine sample was able to reach 300 % elongation at break with a tensile strength of 7.56 MPa and Young's modulus of 11.5 MPa, while the self-healed sample was able to reach 370 % elongation at break with a tensile strength of 7.87 MPa and Young's modulus of 7.84 MPa which shows excellent recovery (Figure 5c), further indicating the excellent self-healing properties of FBE15. Furthermore, the self-healing capabilities of FBE15 under water was investigated by cutting and healing another 4 cm strip of FBE15 for 5 min while immersed in water. To account for the changes to the mechanical properties due to being immersed in water, a pristine sample was also immersed in water for the same duration. The sample healed under water was able to stretch to 130 % of its original length before breakage (Figure 5b), and tensile tests shows that it could reach 660 % elongation at break with a tensile strength of 1.15 MPa and Young's modulus of 1.71 MPa, compared to the pristine sample under water which reached 530 % elongation at break with a tensile strength of 1.33 MPa and Young's modulus of 0.85 MPa (Figure 5d).

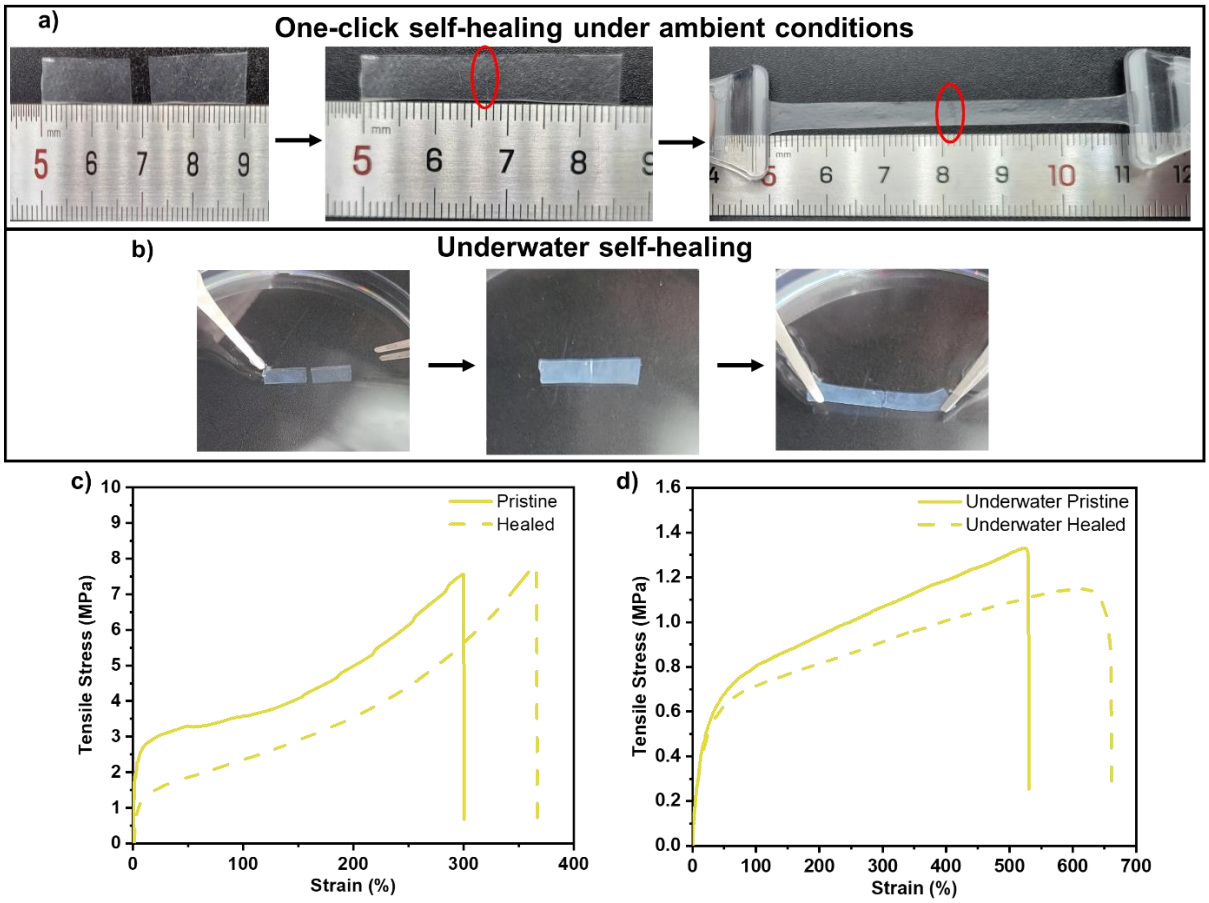

Figure 5. Self-healing demonstration of FBE15. (a) Cut FBE15 stretched to 150 % of original length, immediately after being pressed together; (b) Underwater self-healing demonstration of FBE15 stretched to 130 % after healing for 5 min in water; (c) Tensile test of pristine (solid line) and healed FBE15 (dash line) after 5 min; (d) Tensile test of pristine (solid line) and self-healed (dash line) FBE15 samples under water after 5 min.

To determine the effects of introducing -CF_3 moieties into the material, a control material (HBE15) was synthesized in a similar manner by replacing TFEA monomer with ethyl acetate instead. Both FBE15 and HBE15's self-healing was observed on a microscopic scale by making a 100 µm cut along the material surface and recording the damaged section after 15 min. While FBE15 was able to completely heal from damage after 15 min (Figure 6a & S4),

there was no reduction observed in the HBE15 sample (Figure 6b), indicating a poorer self-healing capability of HBE15 compared to FBE15. DSC and DMA analysis was also conducted on HBE15, which shows similar thermal and thermochemical behavior compared to FBE15 (Figure 6c & S5). However, the time taken for HBE15 to relax from the applied strain of 10 % at room temperature was significantly slower (9 min vs 1 min). Hence, the inclusion of -CF_3 side chains is essential for the rapid self-healing observed in FBE15.

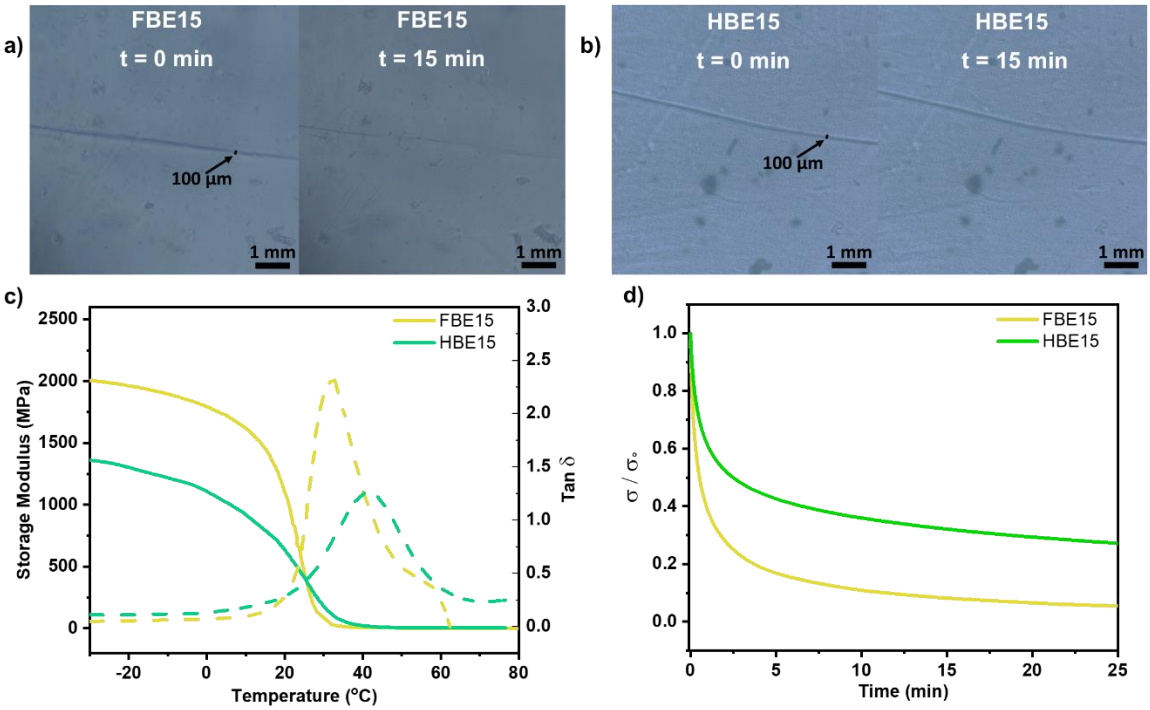

Figure 6. Comparison of FBE15 and HBE15. (a) Microscopic images of FBE15 at 0 min (left) and 15 min (right) after a 100 µm damage was induced with a knife (20x magnification); (b) Microscopic images of HBE15 at 0 min (left) and 15 min (right) after damage was induced with a knife (20x magnification); (c) Plot of storage modulus and tan δ against temperature of FBE15 (yellow) and HBE15 (green); (d) Stress relaxation of FBE15 (yellow) and HBE15 (green)at 25 °C.

To elucidate the contributing effect of the -CF_3 moiety in accelerating the self-healing effect, molecular electrostatic potential (ESP) mapping was utilized as a method for identifying prospective binding sites on the polymer (Figure 7a). Conventionally, regions characterized by relatively positive ESP engender nucleophilic reaction sites, whereas those with a more negative ESP are inclined to electrophilic reactions. Notably, the integration of a -CF_3 group in FBE15 notably enhances the positive ESP of the adjacent -CH_2 group, particularly in comparison to its -CH_3 group counterpart in HBE15, which increases the interaction between the polymer chains. This nuanced discovery implies that polymers modified with -CF_3 may exhibit augmented binding affinities relative to those incorporating -CF_3 groups. The IGMH methodology was also applied to decipher the intricate structural dynamics occurring between FBE15 and HBE15 (Figure 7b). The dipole interactions in FBE15 was discernibly more robust with a binding energy of -7.11 Kcal/mol than that in HBE15 which was only -5.51 Kcal/mol. Furthermore, a comparative evaluation reveals that the binding energy between polymer chains associated with FBE15 markedly supersedes that of HBE15. This empirical evidence, fortified by both the IGMH analysis and meticulous binding energy assessments, implies a potential for a much faster healing rate in the FBE15 compared to the HBE15.

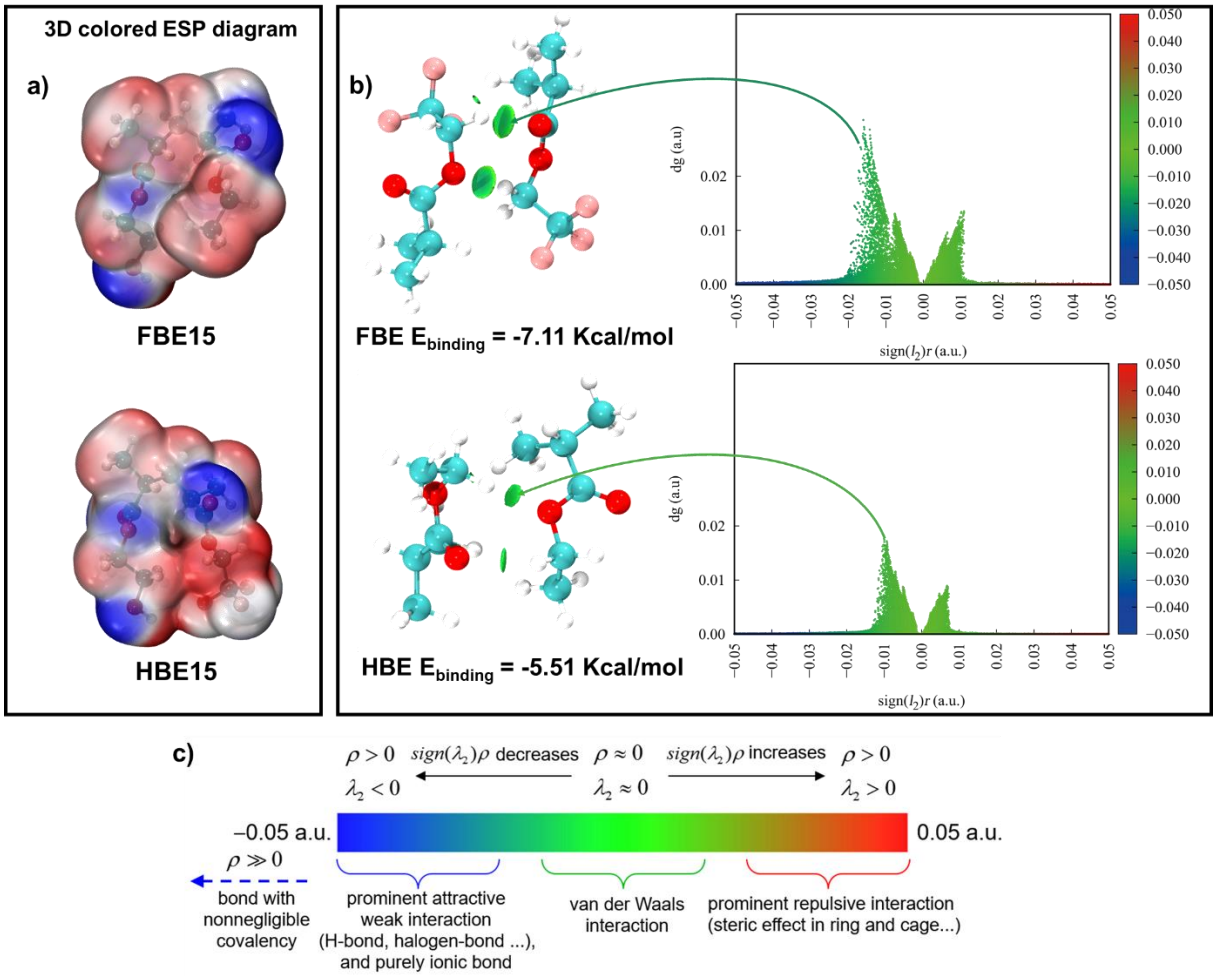

Figure 7. (a) 3D colored ESP diagram of the FBE15 and HBE15 (hydrogen in white, oxygen in red, carbon in cyan, fluorine in pink); (b) scatter map between IGMH and sign(I_2)ρ and isosurface map of IGMH interaction between FBE15 (top) and HVBE (bottom) (hydrogen in white, oxygen in red, carbon in cyan, fluorine in pink); (7c) Common interpretation of coloring method in IGMH maps.

2.5 Closed-loop recycling of FBE15

With the incorporation of dynamic boronic ester bonds in FBE15, the material can be mechanically reprocessed or chemical recycled at the end of its service lifespan (Figure 8). To demonstrate its mechanical reprocessing, 2 g of FBE15 was cut into small pieces and mechanically reprocessed under a hot-press at 40 °C and 5 bar for 15 min, reforming a single intact film similar to the original, with FTIR analysis showing that no significant changes have

occurred (Fig 8d). Tensile tests of the reprocessed film showed a very similar stress-strain curve to the original with 270 % elongation at break with a tensile strength of 7.33 MPa and Young's modulus of 1.38 MPa (Fig 8e). For chemical recycling, FBE15 can be degraded into LFP15 and 1,4-phenylenebisboronic acid by dissolving it in a green solvent containing a mixture of 50 % ethyl acetate / water, stirring it for 4 h at room temperature, and centrifuging at 5000 rpm for 5 min through the hydrolysis of boronic ester bonds. The organic layer with the polymer and residual 1,4-phenylenebisboronic acid is decanted, and the process is repeated for four more times to obtain pure LFP15 after drying which was similar to the original LFP15 in molecular weight, and also in ^{1}H NMR characterization (Figure 8a & 8b), while only 1,4-phenylenebisboronic acid remains in the aqueous layer each cycle and can be dried to obtain pure 1,4-phenylenebisboronic acid which was shown to be the same as a pure sample based on ^{1}H NMR (Figure S5). This method allows 78 % recovery of LFP15 which can be further fabricated into a new FBE15 elastomer by addition of 1,4-phenylenebisboronic acid as a cross-linker (Figure S7). The FBE15 formed from recycled LFP15 shows no significant changes in the FTIR spectrum, and a similar stress-strain curve comparable to the original was also obtained (Figure 8d & 8e). The easy reprocessability and chemical recycling of FBE elastomer in green solvents show great potential of the materials circularity in sustainable applications.

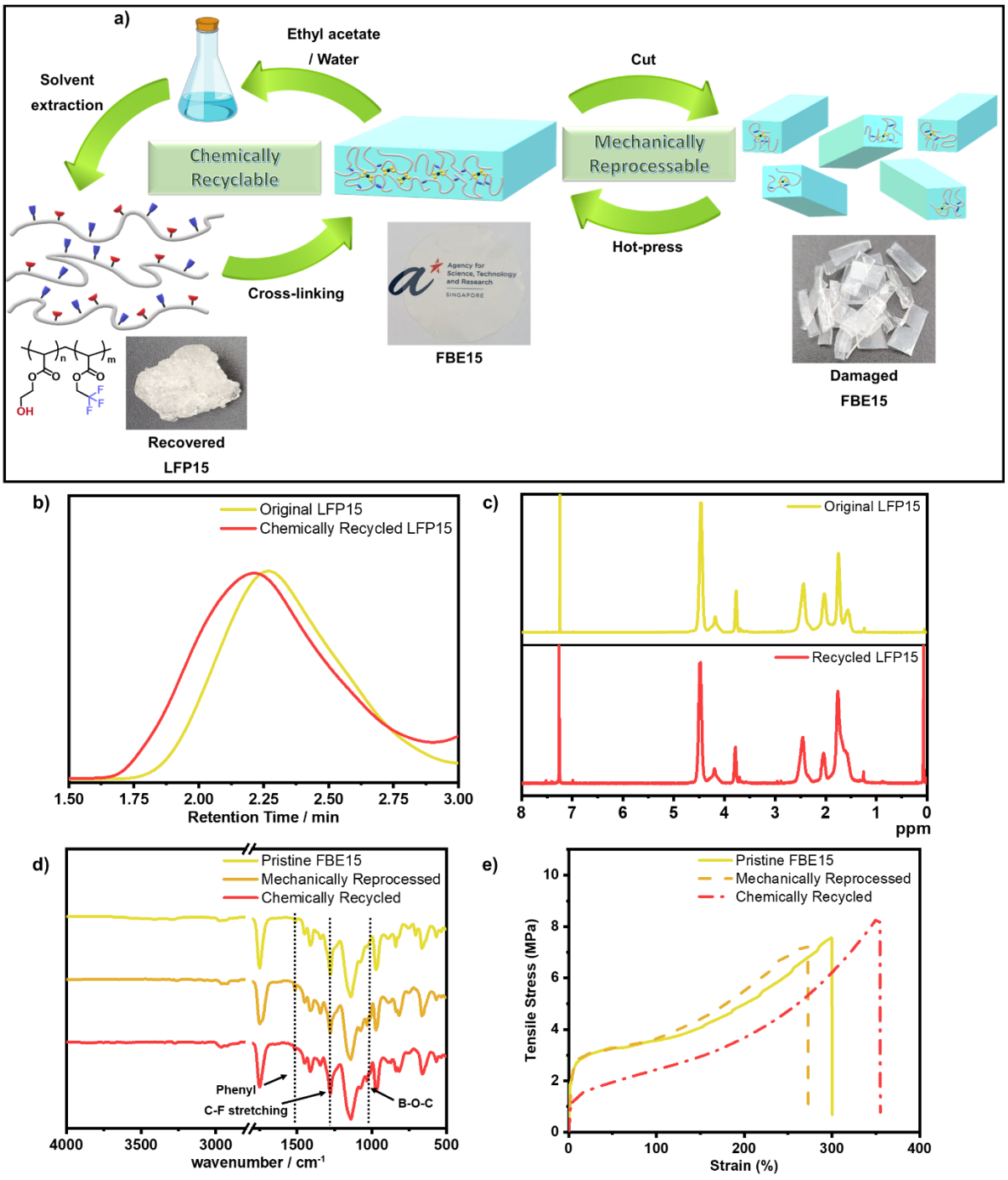

Figure 8. (a) Closed loop recycling of FBE15 by mechanical reprocessing and chemical recycling; (b) GPC trace of original LFP15 and chemically recycled LFP15 (THF eluent, 1.0 mL / min flow rate, 40 °C column temperature, polystyrene standard); (c) ^{1}H NMR spectrum of original LFP15 and recycled LFP15 in $CDCl_3$ solvent; (e) FTIR analysis comparison for pristine, mechanically reprocessed and chemically recycled FBE15 (top: pristine, middle:

mechanically reprocessed, bottom: chemically recycled); (f) Tensile test comparison for pristine, mechanically reprocessed and chemically recycled FBE15 (top: pristine, middle: mechcanilly reprocessed, bottom: chemically recycled).

3. Conclusion

To conclude, we have designed a fluorinated elastomer FBE15 containing both dipole–dipole interaction of -CF_3 side chains together with dynamic boronic ester linkages, which was able to achieve rapid one-click self-healing in the bulk FBE15 material. The thermal and thermomechanical properties of the FBE15 were thoroughly investigated and found to support the excellent self-healing capabilities observed, with the increased efficiency attributed to the increased interaction afforded by the -CF_3 modification In addition, we demonstrated that FBE that reached its end-of-lifespan can be mechanically reprocessed and also be recycled in green solvents in a closed-loop manner yielding the constituent LFP and cross-linker separately, which showed no significant difference to the original polymer and cross-linker. The recycled LFP could be used to refabricate new pristine FBE15 which displayed mechanical properties similar to the original. The excellent self-healing properties and closed-loop reprocessing and recycling afforded by FBE15 makes it a valuable material and is a key step towards circular materials development and sustainable applications.

References

(1) Patrick, J. F.; Robb, M. J.; Sottos, N. R.; Moore, J. S.; White, S. R. Polymers with autonomous life-cycle control. *Nature* **2016**, *540* (7633), 363-370.

(2) Kang, J.; Tok, J. B. H.; Bao, Z. Self-healing soft electronics. *Nature Electronics* **2019**, *2* (4), 144-150.

(3) Qi, M.; Yang, R.; Wang, Z.; Liu, Y.; Zhang, Q.; He, B.; Li, K.; Yang, Q.; Wei, L.; Pan, C.; et al. Bioinspired Self-healing Soft Electronics. *Advanced Functional Materials* **2023**, *33* (17), 2214479.

(4) Tamate, R.; Hashimoto, K.; Horii, T.; Hirasawa, M.; Li, X.; Shibayama, M.; Watanabe, M. Self-Healing Micellar Ion Gels Based on Multiple Hydrogen Bonding. *Advanced Materials* **2018**, *30* (36), 1802792.

(5) Faghihnejad, A.; Feldman, K. E.; Yu, J.; Tirrell, M. V.; Israelachvili, J. N.; Hawker, C. J.; Kramer, E. J.; Zeng, H. Adhesion and Surface Interactions of a Self-Healing Polymer with Multiple Hydrogen-Bonding Groups. *Advanced Functional Materials* **2014**, *24* (16), 2322-2333.

(6) Cao, J.; Lu, C.; Zhuang, J.; Liu, M.; Zhang, X.; Yu, Y.; Tao, Q. Multiple Hydrogen Bonding Enables the Self-Healing of Sensors for Human–Machine Interactions. *Angewandte Chemie International Edition* **2017**, *56* (30), 8795-8800.

(7) Wang, Z.; Ren, Y.; Zhu, Y.; Hao, L.; Chen, Y.; An, G.; Wu, H.; Shi, X.; Mao, C. A Rapidly Self-Healing Host–Guest Supramolecular Hydrogel with High Mechanical Strength and Excellent Biocompatibility. *Angewandte Chemie International Edition* **2018**, *57* (29), 9008-9012.

(8) Hou, J.-B.; Zhang, X.-Q.; Wu, D.; Feng, J.-F.; Ke, D.; Li, B.-J.; Zhang, S. Tough Self-Healing Elastomers Based on the Host–Guest Interaction of Polycyclodextrin. *ACS Applied Materials & Interfaces* **2019**, *11* (12), 12105-12113.

(9) Nakahata, M.; Takashima, Y.; Yamaguchi, H.; Harada, A. Redox-responsive self-healing materials formed from host–guest polymers. *Nature Communications* **2011**, *2* (1), 511.

(10) Mozhdehi, D.; Ayala, S.; Cromwell, O. R.; Guan, Z. Self-Healing Multiphase Polymers via Dynamic Metal–Ligand Interactions. *Journal of the American Chemical Society* **2014**, *136* (46), 16128-16131.

(11) Rao, Y.-L.; Chortos, A.; Pfattner, R.; Lissel, F.; Chiu, Y.-C.; Feig, V.; Xu, J.; Kurosawa, T.; Gu, X.; Wang, C.; et al. Stretchable Self-Healing Polymeric Dielectrics Cross-Linked Through Metal–Ligand Coordination. *Journal of the American Chemical Society* **2016**, *138* (18), 6020-6027.

(12) Li, C.-H.; Zuo, J.-L. Self-Healing Polymers Based on Coordination Bonds. *Advanced Materials* **2020**, *32* (27), 1903762.

(13) Cash, J. J.; Kubo, T.; Bapat, A. P.; Sumerlin, B. S. Room-Temperature Self-Healing Polymers Based on Dynamic-Covalent Boronic Esters. *Macromolecules* **2015**, *48* (7), 2098-2106.

(14) Cromwell, O. R.; Chung, J.; Guan, Z. Malleable and Self-Healing Covalent Polymer Networks through Tunable Dynamic Boronic Ester Bonds. *Journal of the American Chemical Society* **2015**, *137* (20), 6492-6495.

(15) Deng, C. C.; Brooks, W. L. A.; Abboud, K. A.; Sumerlin, B. S. Boronic Acid-Based Hydrogels Undergo Self-Healing at Neutral and Acidic pH. *ACS Macro Letters* **2015**, *4* (2), 220-224.

(16) Ding, X.; Li, G.; Zhang, P.; Jin, E.; Xiao, C.; Chen, X. Injectable Self-Healing Hydrogel Wound Dressing with Cysteine-Specific On-Demand Dissolution Property Based on Tandem Dynamic Covalent Bonds. *Advanced Functional Materials* **2021**, *31* (19), 2011230.

(17) He, L.; Szopinski, D.; Wu, Y.; Luinstra, G. A.; Theato, P. Toward Self-Healing Hydrogels Using One-Pot Thiol–Ene Click and Borax-Diol Chemistry. *ACS Macro Letters* **2015**, *4* (7), 673-678.

(18) Zhou, B.; Deng, T.; Yang, C.; Wang, M.; Yan, H.; Yang, Z.; Wang, Z.; Xue, Z. Self-Healing and Recyclable Polymer Electrolyte Enabled with Boronic Ester Transesterification for Stabilizing Ion Deposition. *Advanced Functional Materials* **2023**, *33* (13), 2212005.

(19) Jing, B. B.; Evans, C. M. Catalyst-Free Dynamic Networks for Recyclable, Self-Healing Solid Polymer Electrolytes. *Journal of the American Chemical Society* **2019**, *141* (48), 18932-18937.

(20) Wang, H.; Shi, Z.; Guo, K.; Wang, J.; Gong, C.; Xie, X.; Xue, Z. Boronic Ester Transesterification Accelerates Ion Conduction for Comb-like Solid Polymer Electrolytes. *Macromolecules* **2023**, *56* (6), 2494-2504.

(21) Li, X.; Yu, R.; He, Y.; Zhang, Y.; Yang, X.; Zhao, X.; Huang, W. Self-Healing Polyurethane Elastomers Based on a Disulfide Bond by Digital Light Processing 3D Printing. *ACS Macro Letters* **2019**, *8* (11), 1511-1516.

(22) Kim, S.-M.; Jeon, H.; Shin, S.-H.; Park, S.-A.; Jegal, J.; Hwang, S. Y.; Oh, D. X.; Park, J. Superior Toughness and Fast Self-Healing at Room Temperature Engineered by Transparent Elastomers. *Advanced Materials* **2018**, *30* (1), 1705145.

(23) Terryn, S.; Brancart, J.; Roels, E.; Verhelle, R.; Safaei, A.; Cuvellier, A.; Vanderborght, B.; Van Assche, G. Structure–Property Relationships of Self-Healing Polymer Networks Based on Reversible Diels–Alder Chemistry. *Macromolecules* **2022**, *55* (13), 5497-5513.

(24) Oehlenschlaeger, K. K.; Mueller, J. O.; Brandt, J.; Hilf, S.; Lederer, A.; Wilhelm, M.; Graf, R.; Coote, M. L.; Schmidt, F. G.; Barner-Kowollik, C. Adaptable Hetero Diels–Alder Networks for Fast Self-Healing under Mild Conditions. *Advanced Materials* **2014**, *26* (21), 3561-3566.

(25) Mah, J. J. Q.; Wang, C.-G.; Surat'man, N.; Solco, S. F. D.; Suwardi, A.; Wang, S.; Loh, X. J.; Li, Z. Metal-Free Synthesis of Biobased Polyisoxazolines toward Sustainable Circular Materials. *ACS Applied Polymer Materials* **2023**, *5* (9), 6747-6752.

(26) Wang, S.; Wang, N.; Kai, D.; Li, B.; Wu, J.; Yeo, J. C. C.; Xu, X.; Zhu, J.; Loh, X. J.; Hadjichristidis, N.; et al. In-situ forming dynamic covalently crosslinked nanofibers with one-pot closed-loop recyclability. *Nature Communications* **2023**, *14* (1), 1182.

(27) Chao, A.; Negulescu, I.; Zhang, D. Dynamic Covalent Polymer Networks Based on Degenerative Imine Bond Exchange: Tuning the Malleability and Self-Healing Properties by Solvent. *Macromolecules* **2016**, *49* (17), 6277-6284.

(28) Wang, P.; Yang, L.; Dai, B.; Yang, Z.; Guo, S.; Gao, G.; Xu, L.; Sun, M.; Yao, K.; Zhu, J. A self-healing transparent polydimethylsiloxane elastomer based on imine bonds. *European Polymer Journal* **2020**, *123*, 109382.

(29) Kathan, M.; Kovaříček, P.; Jurissek, C.; Senf, A.; Dallmann, A.; Thünemann, A. F.; Hecht, S. Control of Imine Exchange Kinetics with Photoswitches to Modulate Self-Healing in Polysiloxane Networks by Light Illumination. *Angewandte Chemie International Edition* **2016**, *55* (44), 13882-13886.

(30) Zhao, Y.; Qin, T.; Jiang, C.; Li, J.; Xiong, Y.; Liu, S.; Qin, J.; Shi, X.; Zhang, G. Boronic ester-based vitrimeric methylvinyl silicone elastomer with "solid-liquid" feature and rate-dependent mechanical performance. *Polymer* **2023**, *265*, 125545.

(31) Cho, S.; Hwang, S. Y.; Oh, D. X.; Park, J. Recent progress in self-healing polymers and hydrogels based on reversible dynamic B–O bonds: boronic/boronate esters, borax, and benzoxaborole. *Journal of Materials Chemistry A* **2021**, *9* (26), 14630-14655.

(32) Chen, Y.; Tang, Z.; Zhang, X.; Liu, Y.; Wu, S.; Guo, B. Covalently Cross-Linked Elastomers with Self-Healing and Malleable Abilities Enabled by Boronic Ester Bonds. *ACS Applied Materials & Interfaces* **2018**, *10* (28), 24224-24231.

(33) Zych, A.; Tellers, J.; Bertolacci, L.; Ceseracciu, L.; Marini, L.; Mancini, G.; Athanassiou, A. Biobased, Biodegradable, Self-Healing Boronic Ester Vitrimers from Epoxidized Soybean Oil Acrylate. *ACS Applied Polymer Materials* **2021**, *3* (2), 1135-1144.

(34) Kim, C.; Ejima, H.; Yoshie, N. Polymers with autonomous self-healing ability and remarkable reprocessability under ambient humidity conditions. *Journal of Materials Chemistry A* **2018**, *6* (40), 19643-19652, 10.1039/C8TA04769C.

(35) Song, K.; Ye, W.; Gao, X.; Fang, H.; Zhang, Y.; Zhang, Q.; Li, X.; Yang, S.; Wei, H.; Ding, Y. Synergy between dynamic covalent boronic ester and boron–nitrogen coordination: strategy for self-healing polyurethane elastomers at room temperature with unprecedented mechanical properties. *Materials Horizons* **2021**, *8* (1), 216-223, 10.1039/D0MH01142H.

(36) Zhao, Z.-H.; Wang, D.-P.; Zuo, J.-L.; Li, C.-H. A Tough and Self-Healing Polymer Enabled by Promoting Bond Exchange in Boronic Esters with Neighboring Hydroxyl Groups. *ACS Materials Letters* **2021**, *3* (9), 1328-1338.

(37) Zhang, Q.; Niu, S.; Wang, L.; Lopez, J.; Chen, S.; Cai, Y.; Du, R.; Liu, Y.; Lai, J.-C.; Liu, L.; et al. An Elastic Autonomous Self-Healing Capacitive Sensor Based on a Dynamic Dual Crosslinked Chemical System. *Advanced Materials* **2018**, *30* (33), 1801435.

(38) Deng, G.; Li, F.; Yu, H.; Liu, F.; Liu, C.; Sun, W.; Jiang, H.; Chen, Y. Dynamic Hydrogels with an Environmental Adaptive Self-Healing Ability and Dual Responsive Sol–Gel Transitions. *ACS Macro Letters* **2012**, *1* (2), 275-279.

(39) Qu, P.; Lv, C.; Qi, Y.; Bai, L.; Zheng, J. A Highly Stretchable, Self-Healing Elastomer with Rate Sensing Capability Based on a Dynamic Dual Network. *ACS Applied Materials & Interfaces* **2021**, *13* (7), 9043-9052.

(40) Cheng, B.; Lu, X.; Zhou, J.; Qin, R.; Yang, Y. Dual Cross-Linked Self-Healing and Recyclable Epoxidized Natural Rubber Based on Multiple Reversible Effects. *ACS Sustainable Chemistry & Engineering* **2019**, *7* (4), 4443-4455.

(41) Wang, S.; Urban, M. W. Self-Healable Fluorinated Copolymers Governed by Dipolar Interactions. *Advanced Science* **2021**, *8* (17), 2101399.

(42) Vandi, L.-J.; Truss, R.; Veidt, M.; Rasch, R.; Heitzmann, M. T.; Paton, R. Fluorine Mobility During SEM-EDX Analysis: A Challenge for Characterizing Epoxy/Fluoropolymer Interfaces. *The Journal of Physical Chemistry C* **2013**, *117* (33), 16933-16941.

(43) Gosecki, M.; Gosecka, M. Boronic Acid Esters and Anhydrates as Dynamic Cross-Links in Vitrimers. *Polymers* **2022**, *14* (4), 842.

(44) Marco-Dufort, B.; Iten, R.; Tibbitt, M. W. Linking Molecular Behavior to Macroscopic Properties in Ideal Dynamic Covalent Networks. *J Am Chem Soc* **2020**, *142* (36), 15371-15385.

Supporting Information

The supporting information provided contains information on the materials and methods used along with Figures S1 – S7 mentioned in this article.

Conflicts of interest

There are no conflicts to declare.

Acknowledgements

This project is supported by RIE2025 Manufacturing, Trade and Connectivity (MTC) Programmatic Fund (M22K9b0049) and AME Young Individual Research Grants (YIRG) (Grant No. A2084c0168) administrated by A*STAR.